2012-09-01

Characterisation of friction and lubrication regimes in premium tubular connections

Stewart, F

10.1016/j.triboint.2012.04.011
TRIBOLOGY INTERNATIONAL
Elsevier BV

Characterisation of Friction and Lubrication Regimes in Premium Tubular Connections

F. Stewart [1], H. R. Le[1]*, J. A. Williams [2], A. Leech[3], B. Bezensek[3], A. Roberts[3]

[1] School of Marine Science and Engineering, University of Plymouth, United Kingdom

[2] Department of Engineering, University of Cambridge, United Kingdom

[3]Hunting Energy Services UK Ltd, Badentoy Avenue, Portlethen, Aberdeen, United Kingdom

*Corresponding Author (H R Le): Tel - 01752 586172, Fax – 01752 586101

Email – huirong.le@plymouth.ac.uk

Abstract

A friction test rig has been developed to carry out repeated sliding friction tests for premium tubular connections. The test rig enables accurate measurement of friction in various contact regimes which are relevant to the threaded connections between tubular components. Higher load tests can simulate the contact in metal-to-metal seals under very high contact pressures by using perpendicular pin-on-pin tests. The contact in the thread loading flank under intermediate pressures can be simulated by using larger radius coupon-on-coupon tests. The measured coefficient of friction is well correlated with a lubrication parameter combining lubricant film thickness and initial surface roughness.

Keywords: Tubular connection; Bead peening; Boundary lubrication; Friction;

1. INTRODUCTION

In the oil and gas industry pipe strings are sections of pipe which are connected to a flow conduit. These strings transport hydrocarbons from the bottom of the well to the surface and each could be regarded as a long pressure vessel extending from the harsh producing zones to the well head and beyond. The tubular connections are increasingly exposed to harsh down-hole production environment, such exposure is likely to increase as the search for hydrocarbons goes deeper. To maintain working pressures it is important that the connections are fully sealed by applying the correct torque to the threaded pipe connections so that sufficient pre-load is generated in the metal-to-metal seal of a connection.

Connection assembly torque values are heavily dependent on the system's contacts on the seal and thread areas as shown in Fig. 1(a). The coefficient of friction (CoF) can be calculated from the measured make-up torque using full-scale test setup (shown in Fig. 1(b)). The apparatus is made up of three sections: a motor, a torque transducer and a rotation transducer. The motor provides the specimen with rotation and torque. The torque transducer resists the rotational motion and produces an output signal. The rotational transducer produces an output signal which is proportional to the angle through which the specimen is rotated. The make-up torque is dependent on the coefficient of friction according to a well-established torque equation:

$$T = \frac{p_r.d_m}{2}\left(\frac{l + \pi\mu.d_m.\sec\beta}{\pi.d_m - \mu l \sec\beta} + \mu\frac{d_c}{d_m}\right), \quad (1)$$

where p_r is the pre-load on the shoulder, d_m the mean diameter of the thread, d_c the mean diameter of the shoulder, l the lead of the thread, μ the coefficient of friction and β the flank angle of the thread. Tests are usually performed until yielding occurs. The pre-load can then be estimated for given geometry and yield strength so that the coefficient of friction can be extracted from yield torque. Due to the expense of such testing it is not viable to test all combinations of size, weight and grade of steel. Extrapolation is therefore used to obtain torque values for the untested sizes. Extrapolation and interpolation of torque data can become unreliable due to the nonlinear effects of contact pressure, operating speed and surface conditions. Therefore a laboratory test system is desired for product development.

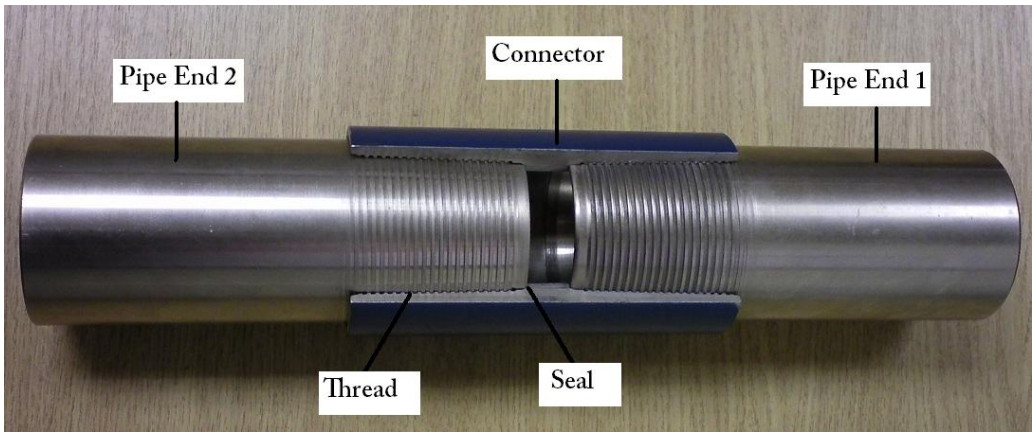

(a)

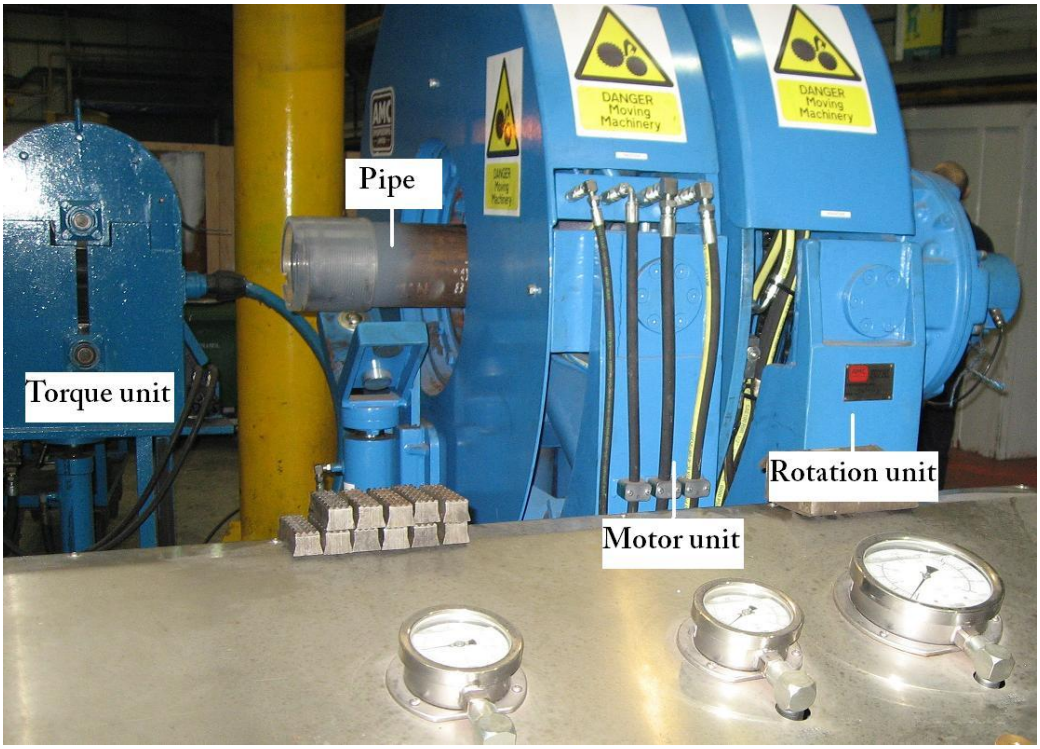

(b)

Figure 1: (a) Elements of a premium pipe connection and (b) pipe connection bucking unit.

Because the coefficient of friction is dependent on the system being tested, it is important that tests carried out in the laboratory are representative of actual field conditions. To measure the coefficient of friction for a so-called premium connection, the main parameters of interest are velocity, sliding distance, contact pressure, surface condition and lubricant.

Various laboratory test methods were reviewed by Podgornik et al [1]. The most simple and widely used procedure for general friction testing is the pin-on-disc method.

In this test, the pin is held stationary and the disc is rotated beneath it generating a circumferential wear track on the disc [2]. Adjustment of pin location is needed to ensure that a new surface of the disc is used each time. A major disadvantage of this set-up is that the speed of the disc must be altered continually to give a steady sliding speed between the pin and disc. There is also difficulty in controlling the surface quality of the usually spherical pin head. This does not always fully represent a real component and is only an idealised and simplified case. Off the shelf pin-on-disc [3] machines usually operate at sliding speeds between 0.05 and 10 m/s which are considerably higher than the rates involved in normal premium connection assembly. If the pin tip is initially spherical then there will be non-conformal contact between the two surfaces generating high pressures which gradually reduce with time and wear [2].

Other geometries commonly used are pin-on-cylinder and crossed cylinder arrangements convenient for point contact because samples can be manufactured with a consistent surface roughness. Carper et al [4] used a conical pin and box with coincident tapers to measure coefficient of friction. The normal load was ramped up while the pin was rotated against the box. The coefficient of friction was extracted from the torque applied and the axial force. This test method requires large axial force to generate required contact pressure and hence large experimental device.

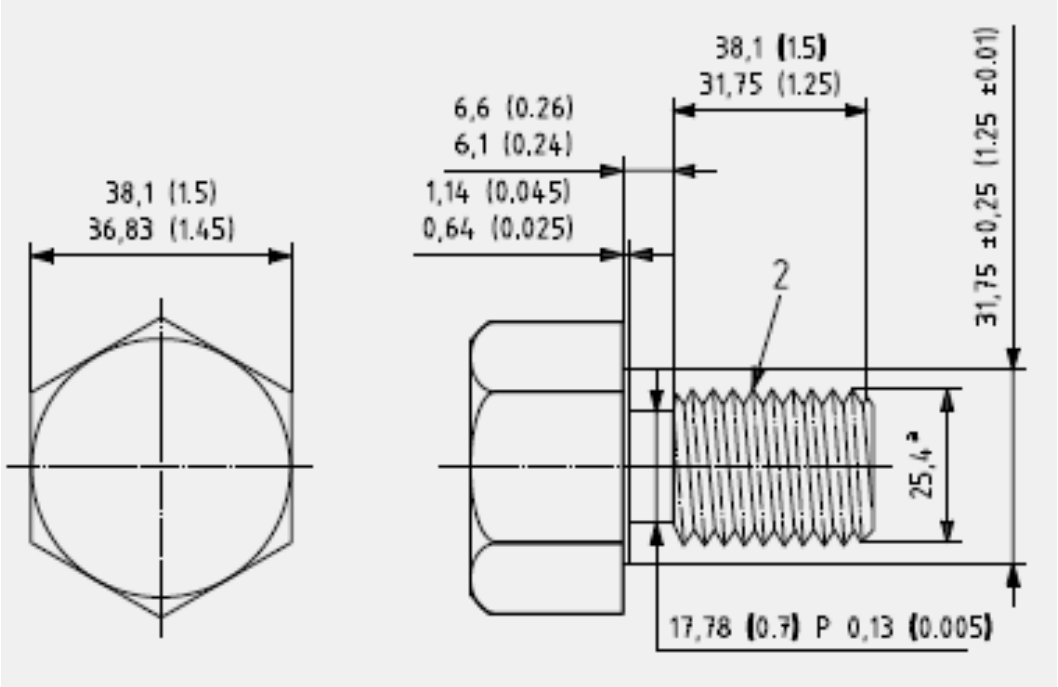

Figure 2: Test 5A3 3rd Edition Test Pieces [5]

One existing method used to test the friction in a premium tubular connection is the nut buster test described in the 3rd Edition of API (American Petroleum Institute) 5A3 Test Procedure [5]. This involves rotating a nut on bolt assembly (shown in Fig. 2) until a specified pre-load is achieved. Coefficients of friction are extracted from the torque data and the estimated contact pressure from the angle of rotation. This is subject to significant error due to the inaccuracy of the dimensions and the assumption of the contact pressure. However, the API test apparatus geometry is also different to that of the connection of interest. The test generates only 200 to 400 MPa (i.e. 30 – 65 ksi) of contact pressure on the loading collar and the average pressure in the threads in these tests is expected to be below 260 MPa (40 ksi). This is significantly lower than the contact pressure on the seal (0.7 – 2 GPa i.e. 100 – 300 ksi), though, according to FEA, is representative of the contact pressure on the threaded section of the connection.

This paper describes the development of a laboratory testing procedure to investigate systematically the effects of premium connection contact pressure, sliding speed, surface conditions and lubricants on the CoF. It includes a case study on an existing commercial system (Clear-Run®) used in today's oil and gas fields which has been developed by Hunting Energy Services in collaboration with MP Eastern and RS Clare [6]. The lubricant used is Clear-Glide which has a viscosity of about 50,000 cP at 25°C. The lubrication regime under these conditions will be analysed using classic lubrication theory.

2. FRICTION TEST RIG

The test rig used in this work is shown in Fig. 3. It was designed so that the samples in the form either of cylinders, of radius 6 mm, or coupons, with a cylindrical surface of radius 60 mm, could be pressed together with their axes at 90°. The upper stationary sample represents the pipe end whilst the lower moving sample represents the coupling. In one configuration the axis of the lower specimen is parallel to its motion so that the contact point on the upper surface remains at rest during the test, as illustrated in Fig. 4(a), while the point of contact moves along the lower cylindrical surface. This configuration simulates the real connection system because during the make-up of the connection, the thread of the pipe is subjected to continuous sliding with the new thread of the coupling. The test can also illustrate the effect of burnishing, by repeated contact, of the top sample.

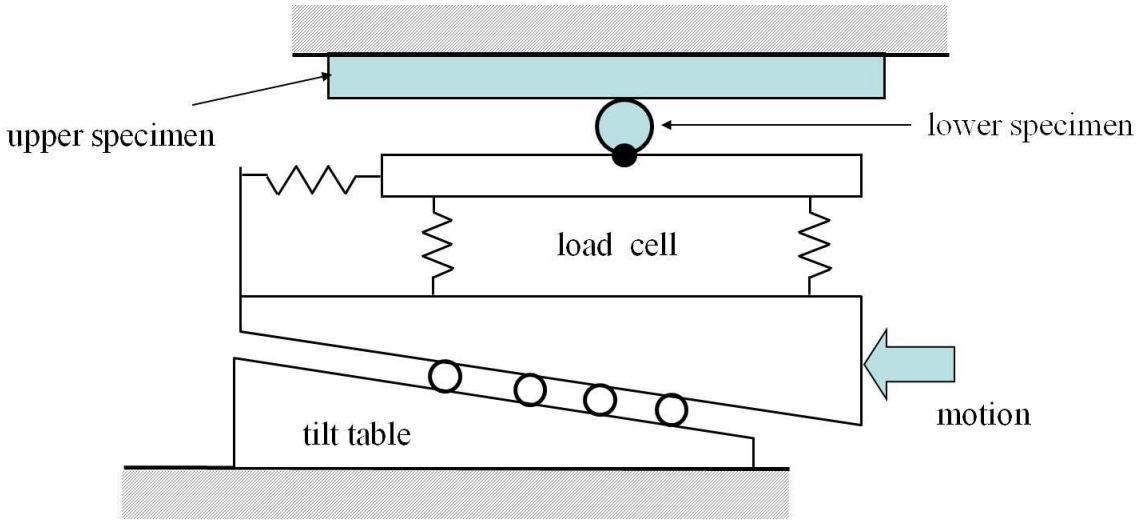

(a)

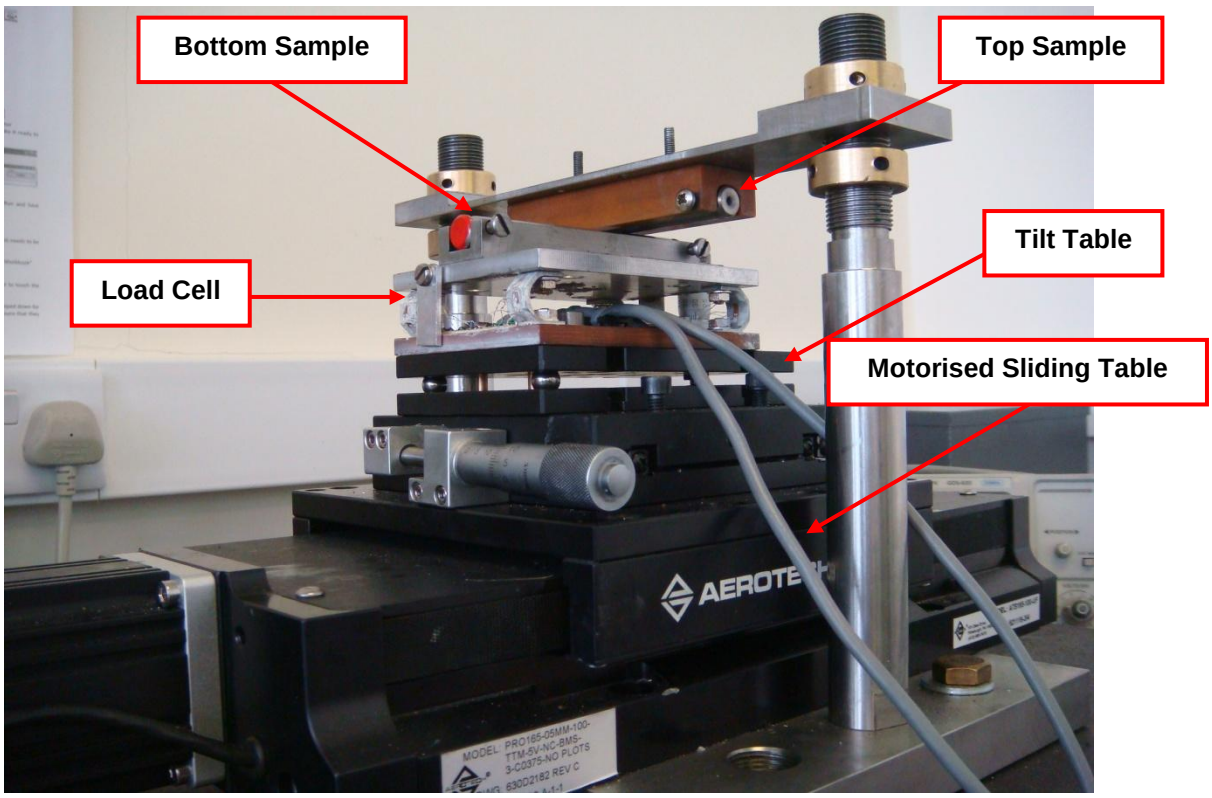

(b)

Figure 3 Cross-cylinder friction and galling test rig set-up (a) schematic (b) embodiment

In an alternative arrangement, the axes of both specimens are inclined at 45° to their motion so that the point of contact between them traces out a linear path on each, as indicated in Fig. 4(b). This can be used to investigate the critical load that causes galling (not investigated here). Only the first cycle exposes the test specimens to a fresh surface, the second and third cycles are executed on the same surface as the first cycle.

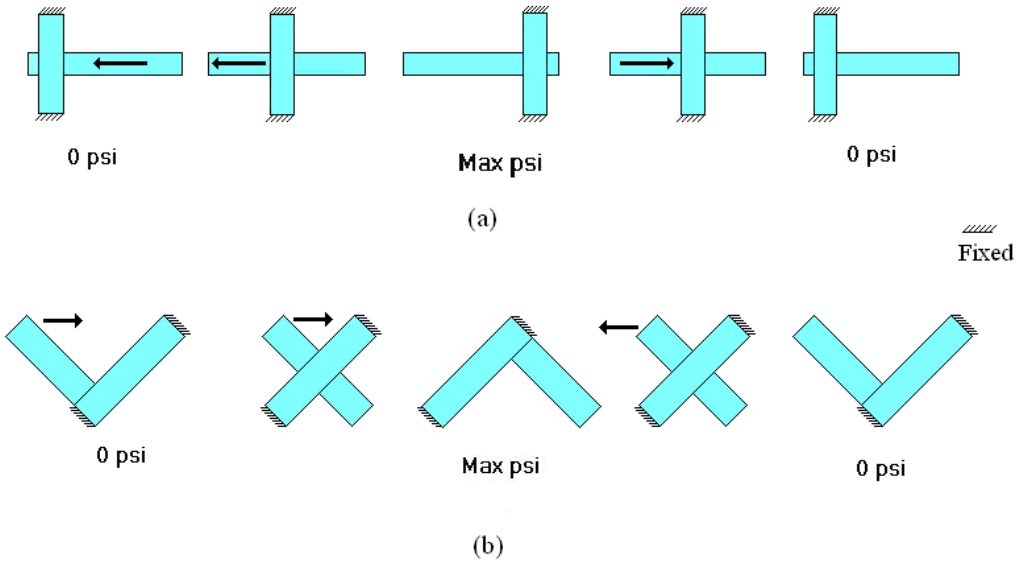

Figure 4: Sample configurations for (a) contact stationary on top sample and (b) contact moving on both samples

In each case, the lower specimen is carried on a stage whose tilt can be adjusted so that the normal load between the specimens increases during the course of the test, see Fig. 3(a). In the present work, each test consisted of a number of cycles, completed consecutively. Lubricant was reapplied between each load cycle to replicate the conditions of the real pipe connection make-up situation.

Both normal force W and tangential force F were measured simultaneously using sixteen strain gauges fixed on the four legs of the specially designed load cell. This is of a similar design to the two component load cell reported previously by the authors [7, 8]. The output normal and tangential voltages were filtered through their respective amplifiers and then fed into a data logging card interfaced with the PC using LabVIEW®. The coefficient of friction is simply defined as the ratio of F to W. Similar work was undertaken by Baragetti et al [9] where strain gauges were mounted on conical threaded connections however this method is much more expensive and gives opportunity for fewer variables.

The load cell was calibrated by applying dead weight loading in the normal and tangential directions and measuring the resultant cross-talk between the two force measuring systems. This was found to increase linearly with load and to be of the order of 12%. A further correction, of the order of 10%, to account for the change of position of the point of application of the load in relation to the load measuring elements of the

dynamometer was also found necessary. Normal loads up to 500 N could be applied and the lower specimen could be traversed at speeds up to 100 mm s^{-1}.

3. EXPERIMENTAL RESULTS

3.1 Pressure regimes

The highest pressure and stress concentration occurring on the final threads and the seal [10] and this must be sufficient to maintain a seal between the mating parts. However, it is also important that this stress does not exceed some maximum value as this can cause plastic deformation and create a leak path [11].

The test samples were machined from commercial 13 Cr steel provided by JFE Steel Co, Japan. Coupons were cut from 13 Cr steel pipes using electrical discharge machining (EDM). The surface roughness of the test surfaces was measured using Zygo 3D surface profile meter. The results are shown in Table I. It is noted that the coupons are much rougher than the pins. This is due to the different machine process. Coupon samples were cut from a pipe with an outer diameter 120mm and inner diameter 100mm. Although the pipe was turned on the same lathe as the pins, the speed and feed rate were different which gave rise to different surface finish. However, each is representative of specific feature in the connection system. The pin has similar surface finish to the seal while the coupon to the thread.

Table I Average surface roughness of test samples

	Regime 1 - Pins			Regime 2 - Coupons		
Surface treatment	As-machined	Ceramic peened	Clear-Plate	As-machined	Ceramic peened	Clear-Plate
Surface roughness, R_a (μm)	0.242	0.308	0.208	0.973	1.063	1.018
Surface roughness, R_q (μm)	0.307	0.405	0.261	1.365	1.748	1.232

Samples were machined into both pins of radius 6 mm and coupons of surface radius 60 mm. This was necessary in order to cover the range of contact pressures required viz. 140 MPa to 2 GPa, i.e. 20 – 300 ksi. The contact conditions between two equal cylinders of radius R crossing at 90° can be thought of as equivalent to those between a sphere of radius $R^* = R/2$ and a plane surface. Thus, on the basis of elastic

contact and smooth surfaces, the mean contact pressure $\bar{p}$, the plane strain modulus E' defined as $E/(1-\nu^2)$ and the normal load W are related by the expression [12],

$$\bar{p} = \frac{1}{\pi}\left(\frac{16WE'^2}{9R^{*2}}\right)^{1/3} \tag{2}$$

The relation between the magnitudes of the applied normal loads and mean contact pressures are as shown in Table II for the two configurations used in the tests i.e. crossed pins and crossed coupons.

Table II Relation between applied normal load and mean contact pressure

	pin-on-pin Regime 1		coupon-on-coupon Regime 2	
Load W (N)	7.9	440	13	593
Mean contact pressure $\bar{p}$ (MPa)	550	2100	140	500

In what follows we refer to the higher pressure tests achieved by using the crossed pin configuration as Regime 1 and the lower pressure tests using the larger radii coupons as Regime 2.

The Clear-Run system used in this work consists of a coating, Clear-Plate®, applied to one of the mating surfaces. The opposing, uncoated surface is conventionally shot peened to reduce the propensity for galling at high interfacial pressures. Before assembly both surfaces are lubricated by an application of a lubricant known as Clear-Glide®. Only a thin layer needs to be applied to both pin and coupling thus reducing the extent of down-hole contamination. The transparency of both elements of the system allows for easy inspection of the threads without having to remove the lubricant. Ceramic beads, stainless steel beads, aluminium oxide and glass particles are commonly used as the peening media.

3.2 Simulation of Clear-Run® system in Regime 1 and Regime 2

For each of these tests, which were run at a sliding speed of $15\,\mathrm{mm\,s^{-1}}$, the Clear-Plate® coated pin was used as the lower specimen which was loaded against an either as-machined or ceramic-peened sample mounted in the top sample holder. In both cases

Clear-Glide® was used as a lubricant. The results for Regime 1 are shown in Fig. 5(a) and (b) in which the coefficient of friction is plotted against the mean contact pressure. Initially, the test was set up to perform three motion cycles (labelled 1, 2 and 3) and the coefficient of friction was determined for both the loading (+) and unloading (-) part of each cycle.

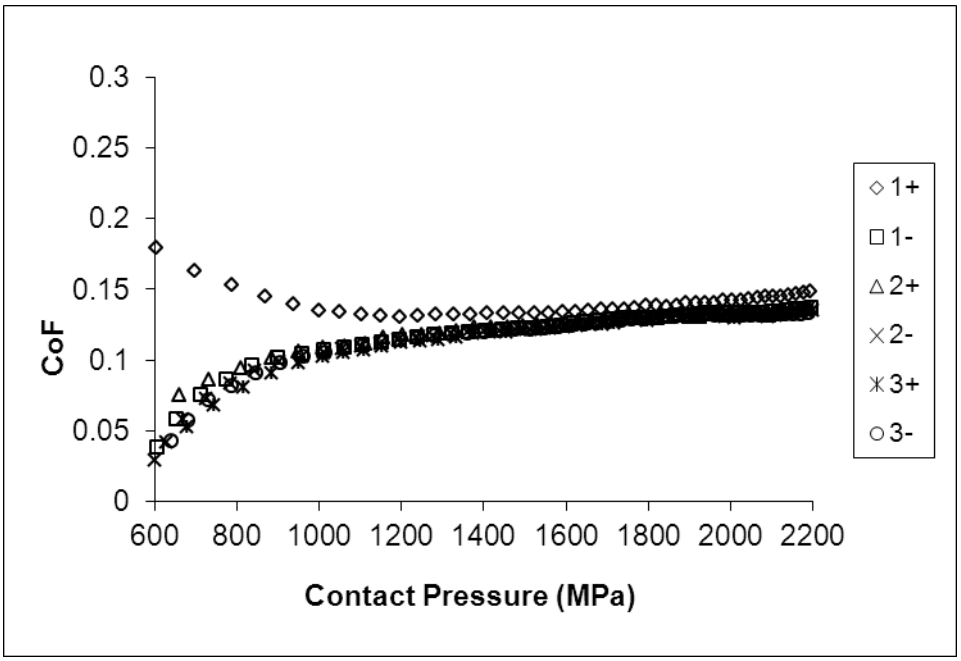

(a)

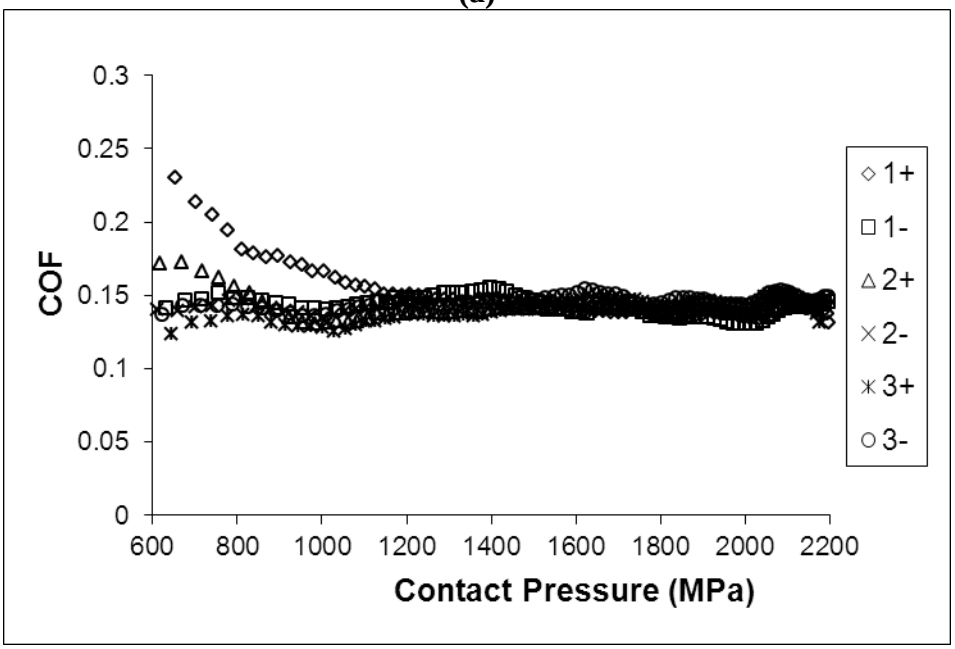

(b)

Figure 5: Comparison between as-machined and ceramic-peened surfaces for regime 1 (600 to 2200 MPa). Tests carried out at 15mm/s with Clear-Glide lubricant, bottom sample made from Clear-Plate and top sample made from (a) As-machined or (b) Ceramic-peened

Images of the samples involved in each combination were taken to compare the wear marks between different materials on the samples after the tests using the 1mm length scale on each photo. Figure 6 shows the Clear-Plate® and ceramic peened samples after the test. These demonstrate that while the peened surface was burnished there was no severe galling or pick-up on or from the Clear-Plate® surface.

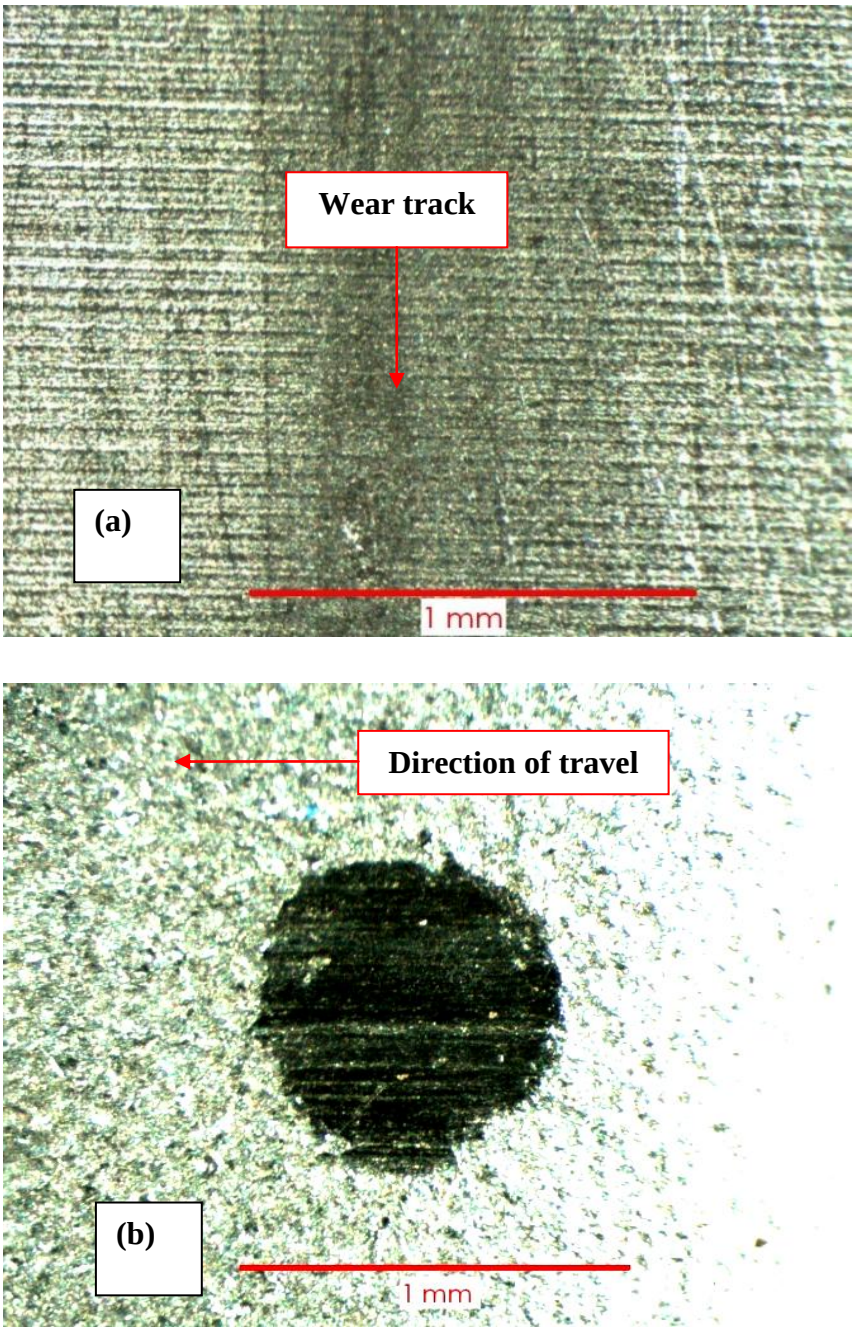

Figure 6 (a) Wear track on Clear-Plate® from test with ceramic peened sample and (b) mark on the ceramic-peened surface

A similar test was repeated for Regime 2 using the perpendicular coupon-on-coupon configuration. Figures 7(a) and (b) show respectively the graphs for coefficient of friction against contact pressure for values between 140 and 500 MPa (20 to 70 ksi) for a ceramic peened surface sliding against an as-machined surface and for one coated with Clear-Plate®.

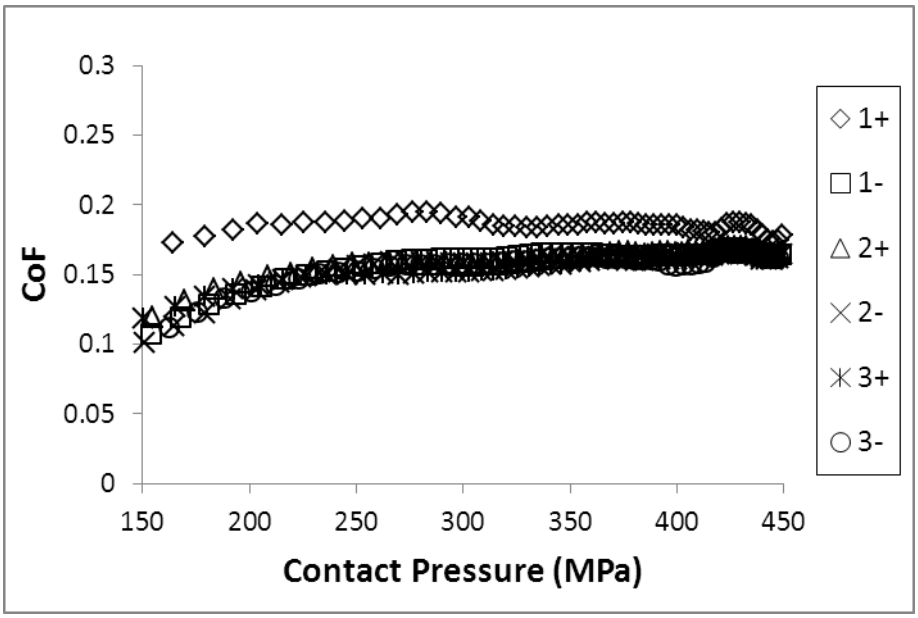

(a)

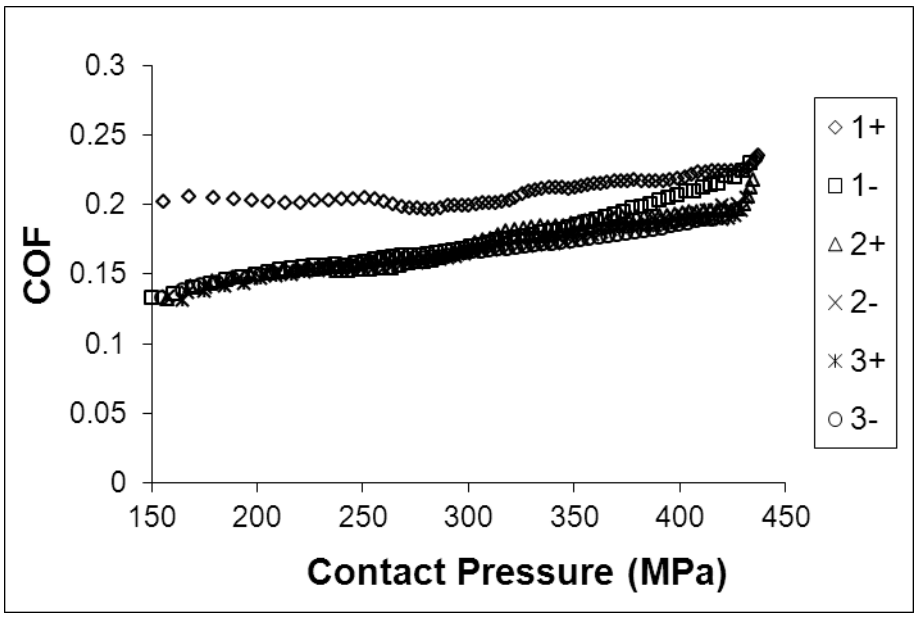

(b)

Figure 7: Comparison between as-machined and ceramic peened surfaces for regime 2 (150 to 450 MPa). Tests performed at 15mm/s with Clear-Glide lubricant, bottom sample made from Clear-Plate and top sample made from (a) as-machined or (b) ceramic-peened

3.3 Effect of initial surface treatments and sliding speed

Figure 8 compares the average coefficient of friction (over the test pressure range) measured using Clear-Plate® coupon surfaces running against either as-machined or shot-peened counterfaces. Both situations were lubricated by Clear-Glide®. Three complete cycles, i.e. 6 strokes, had been performed for each combination at a sliding speed of 15 $\mathrm{mm\,s^{-1}}$. Each CoF value is the average for the pressure range 140 and 500 MPa (20 to 70 ksi). The results showed that CoF decreases by about 20% from the first stroke to the sixth stroke for both conditions. This will be discussed in the next section.

Figure 9 shows a comparison of the effect of both speed and burnishing, i.e. repeated passes, for the ceramic peened Clear-Plate® with Clear-Glide® combination. The graph shows CoF against the cycle number for three different sliding speeds viz. 3, 15 and 50 $\mathrm{mm\,s^{-1}}$. Each test was performed 10 times to find out the effect of burnishing of the surface. The largest difference between the values of CoF is between the first cycle and the second, where the CoF reduces by approximately 20%. This is consistent for the three speeds. After this initial reduction, the coefficient of friction stabilises to a consistent value. The graph also detailed another observation that the sliding velocity affected the average CoF for the system by a notable amount.

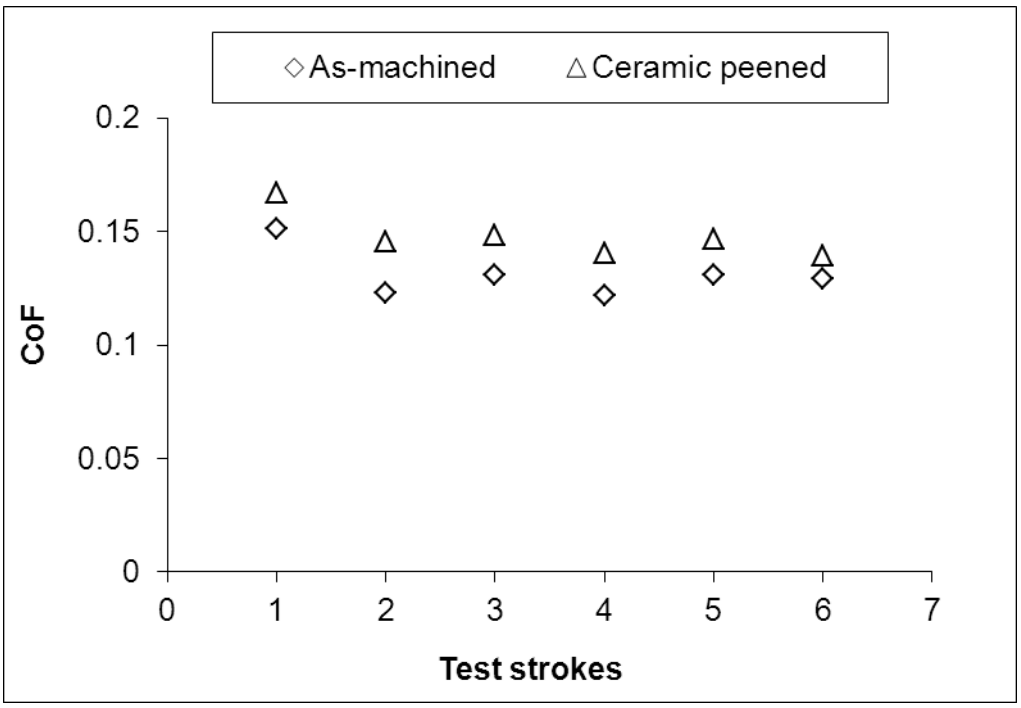

Figure 8: Comparison of as-machined and ceramic-peened coupon tests on Clear-Plated coupon using Clear-Glide lubricant

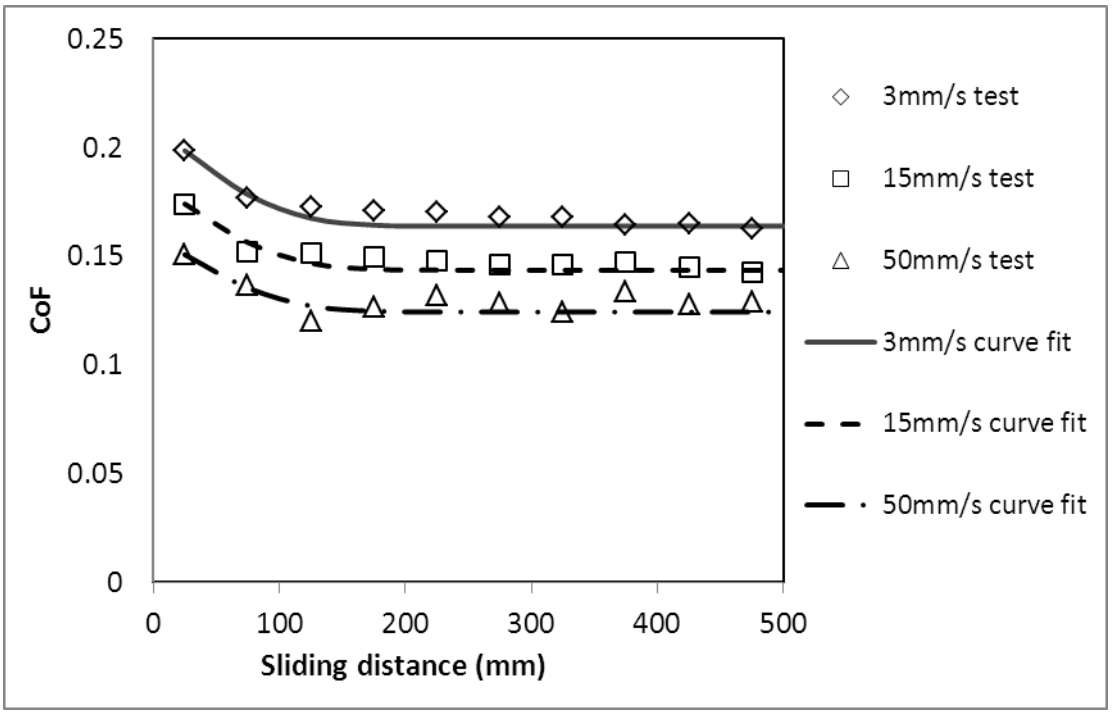

Figure 9: The effects of speed and burnishing on CoF. The curves are best fit to experimental data using the error function

4. DISCUSSION

The results of the tests show that the CoF in the first stroke is always higher than the second stroke (c.f. Figs. 5 and 7). This is similar to the running-in phenomenon observed in piston engine operation in which piston friction decreases with time as the more prominent surface asperities become burnished and so more benign. It is noted that this burnishing effect happens more rapidly in Regime 1 (c.f. Fig. 5) than in Regime 2 (c.f. Fig. 7). This is what one would expect as a result of the contact pressures in Regime 1 being greater than those in Regime 2. According to conventional abrasive wear mechanics[13], the depth t_w of the worn layer is proportional to the applied contact pressure, so that

$$t_w = \frac{K\bar{p}s}{H}, \tag{3}$$

where $\bar{p}$ is the nominal contact pressure, K the non-dimensional wear constant, s the sliding distance and H the material hardness. For the same material and the same wear depth, which might reasonably be associated with the extent of surface burnishing, the

sliding distance required will be inversely proportional to the contact pressure. The surface is therefore burnished more rapidly in the higher pressure Regime 1 tests than in the less severe contacts of Regime 2. It is also noted that the CoF results at higher pressure end of Regime 2 tests are not converging the results of the lower end of Regime 1 tests. This is owing to the very different surface roughness on coupons and pins. They are not directly comparable.

Figure 5 demonstrates the differences in the measured values of the CoF for the as-machined and ceramic peened surfaces under Regime 1. After the initial pass at the higher pressures, both display a CoF of ca. 0.15. However, at the lower values of contact pressure, the CoFs of the as-machined surfaces are significantly lower than those of the ceramic peened specimens. This is an indication of the contribution of hydrodynamic lubrication to the overall resistance to shear. According to Hamrock and Dowson[14], the central lubricant film thickness h_{cen} with a point contact can be derived from the relation

$$h_{cen} = 3.34R\left(\frac{\eta u}{E'R}\right)^{0.64}\left(\frac{W}{E'R^2}\right)^{-0.22}, \tag{4}$$

where η is the viscosity of the lubricant and u the entraining speed (in this case half of the speed of sliding). The lubricant film thickness decreases with increasing load and hence the increase in the 'real' asperity-to-asperity contact ratio. With the ceramic-peened surfaces, the CoF is fairly stable over the whole pressure range. This is typical of boundary lubrication regime. In both cases, the CoF converges to a value of about 0.15 towards the maximum pressure of 2.2 GPa. Tests in Regime 2, Fig. 7, show that the CoF increases with contact pressure for both as-machined and ceramic peened sample. Again this can be associated with the extent of hydrodynamic lubrication. According to equation (4), the lubricant film thickness is proportional to $R^{0.8}$. Even with the larger radius ceramic-peened surfaces, the lubricant film is significant.

The ratio Λ of lubricant film thickness to combined rms surface roughness is often used as a lubrication parameter and given by

$$\Lambda = \frac{h_{cen}}{\sqrt{R_{q,1}^2 + R_{q,2}^2}}, \tag{5}$$

where $R_{q,1}$ is the rms roughness of top surface and $R_{q,2}$ of bottom surface. The values of Λ associated with the current tests are summarised in Table III, based on a sliding velocity of 15 mm s^{-1} and the surface roughness data in Table I.

Table III Lubrication parameter for the tests performed at 15 mm.s^{-1}

	pin-on-pin Regime 1		coupon-on-coupon Regime 2	
Surface treatments	as-machined	ceramic peened	as-machined	ceramic peened
Lamda ratio Λ for W=10N	1.322	1.002	1.783	1.533
Lamda ratio Λ for W=500N	0.426	0.356	0.754	0.648

The average amplitude based on Christensen model of surface roughness [15] is about 3 times the rms roughness. When $\Lambda > 3$, the lubricant film is larger than the average amplitude of surface roughness so that the contact surfaces will be separated by a full or hydrodynamic film. When $\Lambda < 0.3$, the average lubricant film thickness is below a tenth of the amplitude of the surface roughness so that the asperity-to-asperity contact ratio will be large and boundary lubrication will be dominant. Table III indicates that in many cases Λ is larger than 0.3 but below 3.0 so that the lubrication is in the 'mixed' regime. With a maximum load of 500 N in current tests and ceramic peened surface, the Λ ratio is close to 0.3 so that boundary lubrication dominates. On the other hand, with minimum load of 10N and as-machined surface, Λ is much larger so that the hydrodynamic lubrication becomes important.

In the 'mixed' lubrication regime where there is entrapped lubricant as well as asperity-to-asperity contact, the average CoF is a combination of shearing of lubricant and boundary lubrication which can be expressed as

$$\mu = A\mu_b + (1 - A)\mu_v, \tag{6}$$

where the value of $0 < A < 1$ is a measure of the extent of 'real' asperity-to-asperity contact, μ_b is the boundary friction coefficient and μ_v is the CoF in the lubricated region [16]. Because the value of μ_b is likely to be much larger than that of μ_v, which essentially depends on the shearing of lubricant, the average friction increases with

increasing value of the contact ratio A. Under the same lubricant film thickness, the contact ratio A will increase with surface roughness. This explains the results in Fig. 8 showing a higher CoF for tests with ceramic-peened than as-machined surfaces.

Figure 9 confirms that as the sliding velocity increases, the CoF value is reduced. This is again related to the hydrodynamic effect which increases with speed and leads to a thicker lubricant film and hence a reduction in asperity-to-asperity contact. This will reduce the average coefficient of friction according to equation (6).

The effect of burnishing is associated with the gradual removal of surface asperities. As these surface defects are removed, the real asperity-to-asperity contact ratio will decrease and stabilise at a reduced value. A function was determined to give a best-fit curve for CoF versus sliding distance which could fit the trend of CoF from the tests, viz

$$\text{CoF} = \left(0.218 - 0.069\ln(v)\right)\left(1 - 0.171\,erf(z)\right) \tag{7}$$

where v is the sliding velocity and $erf(z)$ is the Guassian error function with

$$z = 4\frac{l - l_1}{l_2 - l_1} \tag{8}$$

in which l is the sliding distance at a particular point, l_1 is the sliding distance of the first stroke and l_2 is the sliding distance when the coefficient of friction stabilises. When l reaches l_2, $z \to 4$ and the value of the error function approaches unity. The comparison in Fig. 9 confirms that this function well describes the variation of friction with sliding distance: the physical justification is similar to the situation described in Kapoor et al [17] which models the influence of surface asperities on the initiation of scuffing.

5. CONCLUSIONS

A cross-cylinder friction test rig has been developed to simulate the sliding friction associated with threaded tubular connections. The test rig allowed for accurate measurement of coefficient of friction up to very high contact pressures under various combinations of surface finish, lubricant, sliding speed.

The test rig enabled measurement of friction in two contact regimes relevant to premium tubular connections: Regime 1 under very high contact pressure 0.6 – 2.2 GPa

(80-300 ksi) using perpendicular pin-on-pin tests and Regime 2 under intermediate pressure 150 – 450 MPa (20-70 ksi) using a perpendicular coupon-on-coupon test.

Test results have confirmed the observations in the field that initial surface treatment significantly affects the coefficient of friction. The burnishing of surface during assembly of tubular connections will significantly affect the stability of friction and thus affect the accuracy of pre-load on the metal-to-metal seal of the connection.

Analysis of lubricant film thickness using Hamrock and Dowson theory and the surface roughness indicates that the lubrication regime is in 'mixed' regime at medium speed. The variation of coefficient of friction with speed, surface roughness and burnishing is well correlated with a lubrication parameter Λ.

ACKNOWLEDGEMENTS

The authors would like to acknowledge the financial support of Hunting Energy Services and TSB through a Knowledge Transfer Partnership grant. Thanks are due to James Forbes and Niall Manzi of Hunting Energy Services and Professor Eric Abel and Steven Clark of the University of Dundee for their help and support for the project. Thanks also to the technical team at the School of Engineering, Physics and Maths of the University of Dundee and the School of Marine Science and Engineering of the University of Plymouth.

REFERENCES

[1] Podgornik B, Hogmark S, Pezdirnik J. Comparison between different test methods for evaluation of galling properties of surface engineered tool surfaces. Wear. 2004;257:843-51.
[2] Williams JA. Engineering tribology. New York: Cambridge University Press; 2005.
[3] Imperial Scientific Industries. Pin on Disc Testers. http://www.tribotesters.com/pin_on_disc.htm; 2011.
[4] Carper HJ, Ertas A, Issa J, Cuvalci O. Effect of Some Material, Manufacturing, and Operating Variables on the Friction Coefficient in Octg Connections. J Tribol-T Asme. 1992;114:698-705.
[5] API Standards Catalogue 5A3, 3rd Edition. Recommended Practice on Thread Compounds for Casing, Tubing, Line Pipe, and Drill Stem: American Petroleum Institute; 2010.
[6] Leech A, Roberts, A., . Development of Dope-Free Premium Connections for Casing and Tubing. SPE Drilling & Completion. 2007;22:106-11.

[7] Le HR, Sutcliffe MPF, Williams JA. Friction and material transfer in micro-scale sliding contact between aluminium alloy and steel. Tribol Lett. 2005;18:99-104.
[8] Le HR, Williams JA, Luo JK. Characterisation of tribological behaviour of silicon and ceramic coatings under repeated sliding at micro-scale. Int J Surf Sci Eng. 2008;2:1-13.
[9] Baragetti S, Clerici P, Matteazzi S. Friction and tightening force of conical threaded connections: experiments in various conditions. Int J Mater Prod Tec. 2003;19:414-30.
[10] Van Wittenberghe J, De Pauw J, De Baets P, De Waele W, Wahab MA, De Roeck G. Experimental determination of the fatigue life of modified threaded pipe couplings. Procedia Engineer. 2010;2:1849-58.
[11] Bradley AB, Nagasaku, S., Verger, E.,. Premium Connection Design, Testing and Installation for HPHT Sour Wells. SPE High Pressure-High Temperature Sour Well Design Applied Technology Workshop. The Woodlands, Texas, USA2005. p. 1-8.
[12] Johnson KL. Contact mechanics. Cambridge Cambridgeshire ; New York: Cambridge University Press; 1985.
[13] Hutchings IM. Tribology : friction and wear of engineering materials: Edward Arnold; 1992.
[14] Hamrock BJ, Dowson D. Elastohydrodynamic Lubrication of Elliptical Contacts for Materials of Low Elastic-Modulus I - Fully Flooded Conjunction. J Lubric Tech-T Asme. 1978;100:236-45.
[15] Christen.H. Some Aspects of Functional Influence of Surface Roughness in Lubrication. Wear. 1971;17:149-&.
[16] Patir N, Cheng HS. Average Flow Model for Determining Effects of 3-Dimensional Roughness on Partial Hydrodynamic Lubrication. J Lubric Tech-T Asme. 1978;100:12-7.
[17] Kapoor A, Williams JA, Johnson KL. The Steady-State Sliding of Rough Surfaces. Wear. 1994;175:81-92.

Figure captions

Fig. 1 (a) Elements of a premium pipe connection and (b) pipe connection bucking unit.

Fig. 2 Test 5A3 3rd Edition Test Pieces

Fig. 3 Cross-cylinder friction and galling test rig set-up (a) schematic (b) embodiment

Fig. 4 Sample configurations for (a) contact stationary on top sample and (b) contact moving on both samples

Fig. 5 Comparison between as-machined and ceramic-peened surfaces for regime 1 (600 to 2200 MPa). Tests carried out at 15mm/s with Clear-Glide lubricant, bottom sample made from Clear-Plate and top sample made from (a) As-machined or (b) Ceramic-peened

Fig. 6 (a) Wear track on Clear-Plate® from test with ceramic peened sample and (b) mark on the ceramic-peened surface

Fig. 7 Comparison between as-machined and ceramic peened surfaces for regime 2 (150 to 450 MPa). Tests performed at 15mm/s with Clear-Glide lubricant, bottom sample made from Clear-Plate and top sample made from (a) as-machined or (b) ceramic-peened

Fig. 8 Comparison of as-machined and ceramic-peened coupon tests on clear-plated coupon using Clear-Glide lubricant

Fig. 9 The effects of speed and burnishing on CoF. The curves are best fit to experimental data using the error function